

This discussion paper is/has been under review for the journal *Climate of the Past* (CP).
Please refer to the corresponding final paper in CP if available.

The last deglaciation: timing the bipolar seesaw

J. B. Pedro^{1,2}, T. D. van Ommen^{1,3}, S. O. Rasmussen⁴, V. I. Morgan^{1,3},
J. Chappellaz⁵, A. D. Moy^{1,3}, V. Masson-Delmotte⁶, and M. Delmotte⁶

¹Antarctic Climate & Ecosystems Cooperative Research Centre, Hobart, Tasmania, Australia

²Institute of Marine and Antarctic Studies, University of Tasmania, Hobart, Tasmania, Australia

³Australian Antarctic Division, Kingston, Tasmania, Australia

⁴Centre for Ice and Climate, University of Copenhagen, Copenhagen, Denmark

⁵Laboratoire de Glaciologie et Géophysique de l'Environnement, Saint Martin d'Hères, France

⁶Laboratoire des Sciences du Climat et de l'Environnement, Saclay, France

Received: 21 January 2011 – Accepted: 21 January 2011 – Published: 26 January 2011

Correspondence to: J. B. Pedro (jbpedro@utas.edu.au)

Published by Copernicus Publications on behalf of the European Geosciences Union.

The last deglaciation: timing the bipolar seesaw

J. B. Pedro et al.

Title Page

Abstract

Introduction

Conclusions

References

Tables

Figures

◀

▶

◀

▶

Back

Close

Full Screen / Esc

Printer-friendly Version

Interactive Discussion



Abstract

Precise information on the relative timing of north-south climate variations is a key to resolving questions concerning the mechanisms that force and couple climate changes between the hemispheres. We present a new composite record made from five well-resolved Antarctic ice core records that robustly represents the timing of regional Antarctic climate change during the last deglaciation. Using fast variations in global methane gas concentrations as time markers, the Antarctic composite is directly compared to Greenland ice core records, allowing a detailed mapping of the inter-hemispheric sequence of climate changes. Consistent with prior studies the synchronized records show that warming (and cooling) trends in Antarctica closely match cold (and warm) periods in Greenland on millennial timescales. For the first time, we also identify a sub-millennial component to the inter-hemispheric coupling: within the Antarctic Cold Reversal the strongest Antarctic cooling occurs during the pronounced northern warmth of the Bølling; warming then resumes in Antarctica during the Intra-Allerød Cold Period i.e. prior to the Younger Dryas stadial. There is little-to-no time lag between climate transitions in Greenland and opposing changes in Antarctica. Our results lend support to fast acting inter-hemispheric coupling mechanisms including recently proposed bipolar atmospheric teleconnections and/or rapid bipolar ocean teleconnections.

1 Introduction

The last deglaciation (ca. 19 to 11 thousand years before present; ka) is the most recent example of a major naturally forced global climate change. Previous studies confirm opposing climate trends on millennial timescales between the northern and southern mid to high-latitudes during this interval (e.g. Sowers and Bender, 1995; Blunier et al., 1998; Blunier and Brook, 2001; Shakun and Carlson, 2010; Kaplan et al., 2010). Antarctica first warmed during the glacial conditions of Greenland stadial 2 (GS-2)

CPD

7, 397–430, 2011

The last deglaciation: timing the bipolar seesaw

J. B. Pedro et al.

Title Page

Abstract

Introduction

Conclusions

References

Tables

Figures



Back

Close

Full Screen / Esc

Printer-friendly Version

Interactive Discussion



then cooled during the Antarctic Cold Reversal (ACR), as Greenland experienced the warmth of the Bølling-Allerød interstadial (B-A or GI-1a-e). Antarctica then resumed warming as Greenland returned to the near-glacial conditions of the Younger Dryas stadial (YD or GS-1).

The conventional explanation for these opposing climate trends is the bipolar ocean seesaw; it proposes that the two hemispheres are coupled via oscillations in the dominant direction of heat transport in the Atlantic Ocean due to perturbations in the meridional overturning circulation (Broecker, 1998). More recently, an alternate (though potentially complimentary) mechanism has been put forward that invokes atmospheric teleconnections in forcing the bipolar coupling (Anderson et al., 2009 and references therein). These two processes, oceanic and atmospheric, differ fundamentally; sorting out their relative roles is critical for understanding Earth's climate dynamics. A key role of the palaeoclimate record is to provide firm observational constraints against which the different theories can be tested.

We begin by constructing a new climate chronology for the last deglaciation from the Law Dome (LD) ice core, Coastal East Antarctica, based on synchronization of fast methane variations at LD with those from Greenland (on the Greenland Ice Core Chronology 2005, GICC05 (Rasmussen et al., 2008). As with all ice core $\delta^{18}\text{O}_{\text{ice}}$ records, the LD record has been interpreted principally as a record of local temperature variations, notwithstanding that $\delta^{18}\text{O}_{\text{ice}}$ may also be influenced by changes in other variables including temperature/humidity at the oceanic moisture source, seasonal distribution of snow fall, surface elevation and anomalous ice flow (e.g. Jones et al., 2009). Construction of composite $\delta^{18}\text{O}_{\text{ice}}$ records from multiple ice cores has been demonstrated previously to reduce these local signals and produce reconstructions that more robustly represent regional climate trends (e.g. White et al., 1997; Andersen et al., 2006a). Therefore, in order to represent climate evolution in the broader Antarctic region, we construct a $\delta^{18}\text{O}_{\text{ice}}$ composite from the LD record and records from other high-accumulation/near-coastal sites: Byrd (Blunier and Brook, 2001), Siple Dome (Brook et al., 2005), Talos Dome (Stenni et al., 2011; Buiron et al., 2011) and EPICA

The last deglaciation: timing the bipolar seesaw

J. B. Pedro et al.

Title Page

Abstract

Introduction

Conclusions

References

Tables

Figures



Back

Close

Full Screen / Esc

Printer-friendly Version

Interactive Discussion



The last deglaciation: timing the bipolar seesaw

J. B. Pedro et al.

Title Page

Abstract

Introduction

Conclusions

References

Tables

Figures

◀

▶

◀

▶

Back

Close

Full Screen / Esc

Printer-friendly Version

Interactive Discussion



Dronning Maud Land (EDML) (EPICA c.m., 2006; Lemieux-Dudon et al., 2010). These five cores are selected since they sample from a wide geographic range, including the Indian (LD), Atlantic (EDML), and Pacific (Siple Dome, Byrd, Talos Dome) sectors of the Antarctic continent (Fig. 1a), and because they can all be methane-synchronized with the GICC05 timescale of the central Greenland ice cores with sufficient accuracy.

The accuracy of the methane synchronization technique is limited by the offset between the age of the ice and the age of bubbles at a certain depth (i.e. the Δ age; a result of the bubbles being sealed off from contact with the atmosphere at a depth of 50–100 m during the transformation of snow to ice). Compared to the cores from the East Antarctic Plateau (e.g. EPICA Dome C (EDC) and Vostok), the relatively high accumulation records used here have more accurately constrained, and lower Δ ages by up to an order of magnitude (Table 1), leading to greater precision in the methane synchronization.

The robust Antarctic-wide climate signal which emerges in the composite is used to provide tighter constraints on the relative timing of north-south climate variations during the deglaciation.

2 Methods

2.1 Construction of the revised LD $\delta^{18}\text{O}_{\text{ice}}$ chronology

The previous LD methane record (Morgan et al., 2002) is supplemented here with additional measurements that improve our timing constraints. Additional $\delta^{18}\text{O}_{\text{ice}}$ measurements were also made on the LD record improving its temporal resolution to an average of 25 yr per sample for the interval 9 ka to 21 ka.

The LD $\delta^{18}\text{O}_{\text{ice}}$ record was placed on the GICC05 timescale by synchronizing the LD CH_4 variations with GISP2 CH_4 variations on the GICC05 time scale. To obtain GISP2 CH_4 on GICC05 the GISP2 CH_4 record on the ss09 time scale (reported in Blunier and Brook., 2001) was linearly interpolated to GRIP depths using the ss09

age-depth relation (Johnsen et al., 1997) and then to GICC05 ages by linear interpolation using stratigraphical markers (Rasmussen et al., 2008).

Figure 2 shows the GISP2 methane record and the new LD methane record. Also shown are the timings of the abrupt onsets of the Bølling, YD and Holocene climate stages, as derived from the stable isotope records of the annually layer counted GRIP, NGRIP and GISP2 ice cores (Rasmussen et al., 2006; Andersen et al., 2006b; Steffensen et al., 2008). The timing of methane transitions is considered to be synchronous with the onsets of these climate stages. The LD gas age scale was tied to GICC05 at the times of these methane transitions. On the older side of the deglaciation, the onset of the slow deglacial rise in methane (through the interval ca. 16 ka to 15 ka) is used as a tie. We also used methane ties to GISP2 during Dansgaard-Oeschger events 7 and 8 (35.48 and 38.22 ka, respectively). On the younger side of the deglaciation we use a $\delta^{18}\text{O}_{\text{air}}$ tie to GISP2 and GRIP (9.30 ka).

The gas age ties were converted to ice age ties by adding an estimate of the difference between the age of the gas and the age of the ice (i.e. the Δage). We estimated Δage using the Pimienta firn densification model (Barnola et al., 1991), which requires temperature and accumulation rate input. Surface temperature was estimated from $\delta^{18}\text{O}_{\text{ice}}$ by scaling of the modern temporal (seasonal) relationship between $\delta^{18}\text{O}_{\text{ice}}$ and temperature (T) at Law Dome ($\delta^{18}\text{O}_{\text{ice}}$ is proportional to $0.44T$) (van Ommen and Morgan., 1997). Accumulation rates and ages between tie points are calculated using a simple Dansgaard-Johnsen flow model, fitted to the chosen age ties, as discussed elsewhere (van Ommen et al., 2004). The model predicts relatively low accumulation rates at Law Dome during the deglaciation, for instance ca. 20% of modern at 15 ka and ca. 10% of modern during the LGM. These model accumulation rates are the most reliable estimate available for LD and they are independently supported by measurements of the deglacial changes in $\delta^{15}\text{N}_{\text{air}}$ at LD (Landais et al., 2006). An alternate method of estimating paleoaccumulation rate from the water vapor pressure (derived from $\delta^{18}\text{O}_{\text{ice}}$) is often used at ice core sites on the East Antarctic Plateau. The water vapor pressure technique is not suited to the Law Dome site where, in contrast to

CPD

7, 397–430, 2011

The last deglaciation: timing the bipolar seesaw

J. B. Pedro et al.

Title Page

Abstract

Introduction

Conclusions

References

Tables

Figures

◀

▶

◀

▶

Back

Close

Full Screen / Esc

Printer-friendly Version

Interactive Discussion



the East Antarctic plateau, the accumulation rate appears to be influenced by cyclonic activity rather than by local temperature controls on the atmospheric moisture content. Problems with the assumed relation between vapor pressure and accumulation are also noted at other near coastal sites (Monnin et al., 2004).

There are two main sources of error in the LD ice age ties: firstly, the uncertainty in our alignment of the fast methane transitions at Law Dome with those at GISP2 (the correlation uncertainty, σ_{correl}), and secondly, the uncertainty in the LD Δage (which we conservatively estimate as $\pm 30\%$ of Δage , $\sigma_{\Delta\text{age}}$). The gas age ties, Δages and ice age ties together with their estimated uncertainties are listed in Table 2. We do not include in our error estimates the uncertainty in the GICC05 timescales for the GISP2 gas age ties; rather, we specify that the error in our age ties is relative to the GICC05 timescale.

2.2 Construction of the Antarctic $\delta^{18}\text{O}_{\text{ice}}$ composite record

In constructing the Antarctic composite, LD, Byrd, Siple Dome, Talos Dome and EDML $\delta^{18}\text{O}_{\text{ice}}$ series on their GICC05 timescales (see Appendix A) were interpolated to 20 yr time steps. Each series was standardized over the interval 9–21 ka to zero mean and unit standard deviation and the mean of the five data sets was taken at each time step. Extension of the composite beyond 21 ka is not possible at this stage due to the lack of fast methane variations or other high-quality inter-hemispheric dating ties with which to synchronize the records. Accordingly, our focus here is only on the deglaciation, i.e. the interval beginning with the onset of a coherent Antarctic warming trend and ending with the termination of the warming trend at the start of the Holocene.

2.3 Statistical analysis of warming and cooling trends

A statistical approach, SiZer analysis of curvature (Chaudhuri and Marron, 1999), is used to objectively determine the timing of significant climate features in both the LD and Antarctic composite $\delta^{18}\text{O}_{\text{ice}}$ records during the deglaciation.

The last deglaciation: timing the bipolar seesaw

J. B. Pedro et al.

Title Page

Abstract

Introduction

Conclusions

References

Tables

Figures

◀

▶

◀

▶

Back

Close

Full Screen / Esc

Printer-friendly Version

Interactive Discussion



The last deglaciation: timing the bipolar seesaw

J. B. Pedro et al.

Title Page

Abstract

Introduction

Conclusions

References

Tables

Figures

⏪

⏩

◀

▶

Back

Close

Full Screen / Esc

Printer-friendly Version

Interactive Discussion



SiZer applies a series of smoothing filters to the time series (Fig. 3a and c) and depicts the sign of the slope as a function of time and filter width (Fig. 3b and d). We define the onset of deglaciation as the time at which a significant warming trend starts, the ACR onset is then bracketed by the *end* of the significant *warming* trend and the *start* of a significant *cooling* trend. Similarly the ACR termination is bracketed by the end of the significant ACR cooling trend and the resumption of a significant warming trend, and the end of the deglaciation is where the significant warming trend ceases.

In using SiZer for the identification of climate features a decision must be made on the smoothing filter width that adequately removes short term noise whilst preserving the major millennial and sub-millennial scale climate features of interest. Hence the optimal smoothing filter width will depend on the level of noise in the record. As it is an individual core, the level of noise in the LD record is expected to be larger than that of the 5-core Antarctic composite.

For the LD record, at smoothing widths > 250 yr only the major millennial and sub-millennial scale features persist, whereas at < 250 yr there are multiple short term variations of questionable significance (Fig. 3b). Therefore we interpret changes in the sign of the slope at a filter width of 250 yr to be significant climate features. For each feature we include an error term which is the sensitivity of the timing to adjusting the smoothing width by ± 50 yr (shown as the horizontal dashed lines in Fig. 3b). For the composite record, in which short term variability is damped with respect to LD, significant climate features are extracted at a smoothing width of 200 y, again we include an error term reflecting sensitivity to ± 50 yr adjustments of the smoothing width (shown as the horizontal dashed lines in Fig. 3d). Additional details are provided in the caption to Fig. 3.

2.4 Dating uncertainty in the Antarctic composite

The dating uncertainty of the Antarctic composite ($\sigma_{\text{Composite}}$) relative to GICC05 includes contributions from the dating uncertainty of the five records ($\sigma_{\text{LD ice}}$, $\sigma_{\text{Byrd ice}}$, $\sigma_{\text{Siple ice}}$, $\sigma_{\text{Talos ice}}$, $\sigma_{\text{EDML ice}}$). In the same way as for $\sigma_{\text{LD ice}}$ (Sect. 2.1), the individual

core σ_{ice} values at Byrd and Siple Dome are calculated (following Blunier and Brook (2001)) as the RMS sum of the methane synchronisation (σ_{correl}) uncertainty and the Δ_{age} uncertainty ($\sigma_{\Delta_{age}}$) reported by the original authors of each record (Blunier and Brook, 2001, and Brook et al., 2005, respectively). For Talos Dome and EDML we adopt the σ_{ice} values reported with the recent publications of GICC05 consistent timescales for those cores (Buiron et al., 2011, and Lemieux-Dudon et al., 2010, respectively). These uncertainty terms are reported in Table 3.

Combining the uncertainties from the individual cores into one uncertainty value for the composite record is not straightforward: firstly, the uncertainties in the individual records vary with time during the deglaciation; secondly, it cannot be assumed that the individual uncertainties are independent; and thirdly, to our knowledge there is no formal way of combining dating uncertainty in individual records into one dating uncertainty for a composite. These complications prevent us providing any formal “standard error” value for the composite. However, a conservative estimate is that the overall uncertainty is lower than the average of the uncertainty of the individual records.

A “jack-knifing” test, in which the composite was constructed by including all and then leaving out one in turn of the five records, was used to test the robustness of the composite dating. The timing of climate features is essentially unchanged when this technique is applied. For instance, in the resulting 6 versions of the composite, the timing of the pre-ACR isotope maximum does not vary *at all* from 14.76 ka. This result supports the robustness of the dating and the presence of a coherent Antarctic-wide climate signal within the five records.

3 Results and discussion

Figure 1b shows the LD ice core oxygen isotope record ($\delta^{18}O_{ice}$) alongside the records from Byrd, Siple Dome, Talos Dome and EDML, all on the common GICC05 timescale. All records show a similar pattern: an overall warming trend interrupted by the millennial scale ACR. However, the precise timing of changes in climate trends differs between

The last deglaciation: timing the bipolar seesaw

J. B. Pedro et al.

Title Page

Abstract

Introduction

Conclusions

References

Tables

Figures



Back

Close

Full Screen / Esc

Printer-friendly Version

Interactive Discussion



closest to the Southern Ocean. Alternately, the dating of the EDC record may be biased to younger ages; concerns have been raised recently about the reliability of Δ age estimates for the EDC ice core during the deglaciation (Loulergue et al., 2007).

Turning now to the relative timing of north-south climate variations, Fig. 5 shows the Antarctic composite and the North Greenland Ice Core Project (NGRIP) $\delta^{18}\text{O}_{\text{ice}}$ record (NGRIP members, 2004) through the period 11–20 ka, interpreted as a proxy for climate in the broader North Atlantic region (hereafter, the “north”). We refrain from constructing a Greenland ice core composite since the main climate transitions (i.e. the transitions defined in the INTIMATE climate event stratigraphy (Lowe et al., 2008) are already simultaneous between the Greenland records when studied at 20 yr time resolution (Rasmussen et al., 2008).

Colored vertical bands in Fig. 5 illustrate significant warming and cooling trends in the Antarctic composite (hereafter the “south”), the timings of these features are also listed in Table 4. Significant millennial scale warming begins in the south at 18.0 ± 0.39 ka. In the north, stadial conditions (GS-2) prevail until the abrupt warming of the Bølling onset at 14.64 ka; it has been previously proposed that the ACR onset also happened at around this time (Blunier and Brook, 2001, EPICA c.m., 2006). However, the issue of which came first (of critical importance in separating cause and effect) is debated (Morgan et al., 2002) and has been complicated by the non-consistent timescales previously used for individual Antarctic cores. Using the composite, we see that the end of the significant deglacial warming trend in the south (at 14.76 ± 0.20 ka) and the start of significant ACR cooling (14.62 ± 0.20 ka) tightly bracket the Bølling onset. This synchrony of trend change in the south with transition in the north supports the view that the two events are coupled.

Progressing through the deglaciation we find evidence for north-south climate coupling on sub-millennial timescales. The period of significant cooling within the ACR (14.62 ± 0.20 ka to 14.08 ± 0.17 ka (dark blue band Fig. 5)) coincides tightly with the pronounced warmth of the Bølling (GI-1e). The coherence of the southern cooling trend during this interval implies that it was communicated relatively rapidly and uniformly

The last deglaciation: timing the bipolar seesaw

J. B. Pedro et al.

[Title Page](#)[Abstract](#)[Introduction](#)[Conclusions](#)[References](#)[Tables](#)[Figures](#)[Back](#)[Close](#)[Full Screen / Esc](#)[Printer-friendly Version](#)[Interactive Discussion](#)

around the Antarctic continent. Numerical models (e.g. Liu et al., 2009) and recent proxy-based observations from a south Atlantic sediment core (Barker et al., 2010) suggest that the pronounced Bølling warmth was associated with an “overshoot” of the AMOC and a southward expansion of the North Atlantic Deepwater cell. During this “overshoot”, when heat release in the North Atlantic was at its strongest, our results suggest that heat flux away from the south was also at its strongest.

The initial Bølling warmth deteriorates through the Allerød and is punctuated by abrupt sub-millennial scale cooling events including the Older Dryas (GI-1d) and the Intra-Allerød Cold Period (IACP or GI-1b) (Fig. 5). Results from a sediment core south of Iceland suggest that these sub-millennial cold events coincide with periods of increased meltwater flux to the North Atlantic (Thornalley et al., 2010). Changes in the trend in the Antarctic composite also occur close to the times of these sub-millennial cold events: significant cooling in the south ends around the time of the Older Dryas in the north and a significant post-ACR warming in the south resumes (at 13.18 ± 0.21 ka) coincident with the onset of the IACP and unambiguously earlier (by 330 ± 210 yr) than the onset of the YD stadial in the north (at 12.85 ka).

This result questions the view (e.g. Denton et al, 2010; Kaplan et al., 2010) that the resumption of southern warming at the end of the ACR was *triggered* by the onset of the YD. Therefore, although the entire Allerød period is generally regarded as a mild climatic period in Greenland, we find that in a bipolar seesaw context, the IACP must be regarded as a cold stage in the north with a corresponding warming in the south. This interpretation is in accordance with the NGRIP $\delta^{18}\text{O}_{\text{ice}}$ values during the IACP that are similar to the glacial values in the 17.5–19 ka period. Nevertheless, the YD does coincide with an interval of maximum and uniform warming around most of the Antarctic continent. The southern warming finally terminates (at 11.68 ± 0.23 ka), synchronous with the abrupt Holocene onset in the north (at 11.65 ka).

Our main results are summarized in Fig. 6: firstly, trend changes in the south are aligned with millennial and/or sub-millennial climate transitions in the north and secondly, the coldest (warmest) stages of the deglaciation in the north are aligned with

The last deglaciation: timing the bipolar seesaw

J. B. Pedro et al.

Title Page

Abstract

Introduction

Conclusions

References

Tables

Figures

◀

▶

◀

▶

Back

Close

Full Screen / Esc

Printer-friendly Version

Interactive Discussion



the intervals of significant warming (cooling) in the south. This opposing climate behavior between the hemispheres is consistent with a bipolar seesaw operating with minimal time lag in the transmission of climate signals between the high latitudes of both hemispheres.

Two different (but not mutually exclusive) mechanisms have previously been advanced to explain north-south climate coupling during the deglaciation. The first calls on the bipolar ocean seesaw, whereby weakening of the AMOC during GS-2 and the YD, due to freshwater discharge into the North Atlantic (Ganopolski and Rahmstorf, 2001; McManus et al., 2004), reduces both northward ocean heat transport and deep-water production in the North Atlantic thereby stimulating deepwater formation and warming in the south (Broecker, 1998). A variant of this first mechanism proposes that the strengthening of the AMOC was forced from the south by freshwater perturbations to the Southern Ocean linked to sea ice retreat (Bianchi and Gersonde, 2004; Knorr and Lohmann, 2003) or freshwater discharge from the Antarctic Ice Sheet (Weaver et al., 2003). However, recent model experiments have questioned the efficacy of such “southern triggers”, suggesting that freshwater forcing in the south may lead to local cooling but has little effect on the strength of the AMOC or on temperatures in the north (Stouffer et al., 2007; Swingedouw et al., 2009). The second mechanism invokes an atmospheric teleconnection, whereby North Atlantic cooling during GS-2 and the YD forces a southward shift of the Intertropical Convergence Zone, which in turn strengthens the southern westerlies and/or displaces them southward (Anderson et al., 2009 and references therein). Under this mechanism, the increased intensity of the westerlies is thought to warm the Southern Ocean and Antarctica through a combination of increased wind-driven upwelling, dissipation of sea ice via northward Ekman transport and increased southward eddy transport of heat (Denton et al., 2010 and references therein).

What can our results say about these mechanisms? When considering bipolar coupling during the deglaciation, division of climate in the North Atlantic into three stages (GS-2, B-A and YD) may be too simplistic; we find evidence that the sub-millennial

The last deglaciation: timing the bipolar seesaw

J. B. Pedro et al.

Title Page

Abstract

Introduction

Conclusions

References

Tables

Figures



Back

Close

Full Screen / Esc

Printer-friendly Version

Interactive Discussion



climate transitions within the B-A (suggested to be linked to freshwater forcing events (Thornalley et al., 2010)) may also couple with climate variations in the south. Importantly, the observed timescales of north-south coupling require a mechanism capable of rapid signal transmission between the hemispheres. Fast-acting atmospheric teleconnections clearly meet this criteria. Rapid signal transmission can also be achieved via oceanic pathways through the action of internal ocean waves (e.g. Masuda et al., 2010). In the conceptual model of Stocker and Johnsen (2003), a rapid, wave-mediated seesaw in the Atlantic is coupled to a Southern Ocean (SO) heat reservoir. Under this “thermal bipolar seesaw”, as soon as the north cools, heat begins accumulating in the south (and vice-versa). Therefore, despite the proposed 1000–1500 yr time constant of the SO heat reservoir, the changes of slope in the south that we observe to accompany the abrupt changes in the north remain consistent with the Stocker and Johnsen (2003) model.

Our observations do not directly resolve the question of northern or southern forcing. Indeed, in a coupled system factors in both hemispheres may be important. Interestingly, the warming trends in at least two of the individual records used in the composite weaken well in advance of the Bølling onset, at LD ca. 15.11 ka and at EDML ca. 16.2 ka (see also Stenni et al., 2011), suggesting that warming in the south prior to the ACR in some parts of the continent may have reached a level at which freshwater and/or temperature forcings linked to sea ice retreat were weakening the overturning in the Southern Ocean and causing the local warming trend to falter. In this context, positive freshwater forcing due to deglacial warming in the south and reduced freshwater forcing at the end of H1 in the north may have superimposed and ultimately *both* contributed to the abrupt strengthening of the AMOC and the synchronous ACR and Bølling onsets. A similar concept was investigated in a recent model experiment (Lucas et al., 2010), which found higher amplitude responses of the AMOC when freshwater forcings of opposite sign were simultaneously applied to the deepwater formation areas in both hemispheres.

The last deglaciation: timing the bipolar seesaw

J. B. Pedro et al.

[Title Page](#)[Abstract](#)[Introduction](#)[Conclusions](#)[References](#)[Tables](#)[Figures](#)[Back](#)[Close](#)[Full Screen / Esc](#)[Printer-friendly Version](#)[Interactive Discussion](#)

4 Conclusions

The composite Antarctic climate record derived here is robust (i.e. insensitive to exclusion of individual records) and reflects coherent circum-Antarctic climate changes through the deglacial period. The well-constrained methane ties allow co-registration of Antarctic and Greenland ice core climate records with a ~ 200 yr uncertainty.

The records confirm the operation of a bipolar temperature seesaw and provide strong evidence that the mechanism involved is rapid and operates over millennial and sub-millennial timescales; Antarctic trend changes are seen as counterparts to each of the events in the Greenland climate sequence from the Bølling and Allerød through to the Younger Dryas and the onset of the Holocene. A key result is that the period of strongest Antarctic cooling directly coincides with the period of greatest northern warmth, the Bølling (GI-1e). The high resolution of the present study indicates that significant Antarctic cooling was largely complete by the start of the sub-millennial Greenland cold stage the Older Dryas (GI-1d). Seemingly in contrast to the bipolar seesaw hypothesis we find that Antarctic warming resumes concurrent with the onset of the Greenland Intra-Allerød Cold Period (IACP, GI-1b) and several hundred years before the onset of the Younger Dryas. In a bipolar seesaw context this result implies that the heat balance between the hemispheres was already tipping toward southern warming as conditions in Greenland deteriorated through the Allerød. Hence, we propose that the late Allerød stages GI-1a and the IACP be regarded as “cold” periods in a seesaw context. The core of the Younger Dryas period however does mark the period of most rapid and uniform Antarctic warming.

The Antarctic composite also provides a useful tool for evaluating the deglacial climate records of individual cores, and specifically, the more weakly dated interior East Antarctic records. For example, the younger ACR onset in the EPICA Dome C record could reflect a lag in propagation from coast to interior, different distal source and transport effects, or it may be attributed to dating uncertainties, the refinement of which could be used to reassess the Δ age and accumulation relationships at these sites.

The last deglaciation: timing the bipolar seesaw

J. B. Pedro et al.

Title Page

Abstract

Introduction

Conclusions

References

Tables

Figures



Back

Close

Full Screen / Esc

Printer-friendly Version

Interactive Discussion



Similarly, individual site differences, such as the early cessation of the warming trend at LD (15.11 ka) argue for local or regional influences. A question which requires further investigation is whether this early signal at LD and also the early break in the warming trend at EDML (16.2 ka) are signs of changing Southern Ocean wind or sea-ice conditions that are precursors to the later abrupt onset of the Bølling and the strong, regionally coherent ACR cooling.

Appendix A

Application of the GICC05 time scale to the Byrd, Siple Dome and EDML records

The Byrd, Siple Dome, Talos Dome and EDML records were dated by previous authors by aligning variations in CH₄ with similar variations in Greenland CH₄ records from the GRIP and GISP2 ice cores. We adopt the previous dating of these records and where necessary (Byrd and Siple Dome) transfer them to the common Greenland GICC05 timescale, as described below.

A1 Byrd

Byrd was previously synchronised with GRIP and GISP2 using fast methane variations (Blunier and Brook, 2001) (data from <http://www.ncdc.noaa.gov/paleo/pubs/blunier2001/blunier2001.html>). We converted the Byrd $\delta^{18}\text{O}_{\text{ice}}$ and CH₄ records on their ss09 timescale to GICC05 in two steps:

1. converting the ss09 Byrd ages to GRIP depths via the ss09 age-depth relation (Johnsen et al., 1997) (data from <http://www.iceandclimate.nbi.ku.dk/data/>);
2. converting GRIP depths to GICC05 ages by linear interpolation between the GICC05 GRIP age-depth ties (Rasmussen et al., 2008) (data from <http://www.iceandclimate.nbi.ku.dk/data/>).

The resulting GICC05 timescale for Byrd $\delta^{18}\text{O}_{\text{ice}}$ was compared with an independent transfer of Byrd onto GICC05 by Thomas Blunier (personal communication, February 2010) and agreed with maximum discrepancy in the interval 9 ka to 21 ka of 36 years and average discrepancy of 3.4 yr.

We adopt the previously reported Byrd Δage and Byrd to GISP2/GRIP CH_4 correlation errors (Blunier and Brook, 2001) (data from: <http://www.sciencemag.org/cgi/content/full/sci;291/5501/109/DC1>). The dating error introduced in the transfer from the GISP2 layer counted depth scale to the GICC05 timescale, is negligible compared to the Δage and correlation errors and is therefore not considered. The RMS sum of the Byrd Δage error and CH_4 correlation error during the early middle and late stages of the deglaciation are listed in Table 3.

The average temporal resolution of the Byrd $\delta^{18}\text{O}_{\text{ice}}$ data for the interval 9 ka to 21 ka was 41 yr.

A2 Siple Dome

Siple Dome was previously synchronised with GISP2 using fast methane variations (data from: <http://nsidc.org/data/waiscores/pi/brook.html>) (Brook et al., 2005). We converted the Siple Dome $\delta^{18}\text{O}_{\text{ice}}$ and CH_4 records, which were reported on the GISP2 layer counted timescale to GICC05 in two steps:

1. converting the Siple Dome ages to GISP2 depths via the GISP2 layer counted depth scale (Meese et al., 1997) (data from: <http://www.ncdc.noaa.gov/paleo/icecore/greenland/summit/document/gispdpth.htm>);
2. converting GISP2 depths to GICC05 ages by linear interpolation between the GICC05 GISP2 age-depth ties (Rasmussen et al., 2008) (data from: <http://www.iceandclimate.nbi.ku.dk/data/>).

We adopt the previously reported Δage and CH_4 correlation errors (Brook et al., 2005) (data from: <http://nsidc.org/data/waiscores/pi/brook.html>). The dating error introduced

The last deglaciation: timing the bipolar seesaw

J. B. Pedro et al.

Title Page

Abstract

Introduction

Conclusions

References

Tables

Figures

◀

▶

◀

▶

Back

Close

Full Screen / Esc

Printer-friendly Version

Interactive Discussion



in the actual transfer from the GISP2 layer counted depth scale to the GICC05 timescale, is negligible compared to the Δ age and correlation errors and is therefore not considered. The RMS sum of the Δ age and CH₄ correlation errors in the Siple Dome data during the early middle and late stages of the deglaciation are listed in Table 3.

The average temporal resolution of the Siple Dome data for the interval 9 ka to 21 ka was 32 yr.

A3 Talos Dome

The Talos Dome timescale (Buiron et al., 2011) is consistent with GICC05. Standard dating errors during the early middle and late stages of the deglaciation are listed in Table 3.

The average temporal resolution of the Talos Dome data for the interval 9 ka to 21 ka was 39 yr.

A4 EDML

The recently revised EDML timescale (Lemieux-Dudon et al., 2010) is consistent with GICC05. The revised EDML timescale, $\delta^{18}\text{O}_{\text{ice}}$ and CH₄ data and standard dating errors were obtained from Benedicte Lemieux-Dudon (personal communication, February 2010). Standard dating errors during the early middle and late stages of the deglaciation are listed in Table 3.

The average temporal resolution of the EDML data for the interval 9 ka to 21 ka was 15 yr.

Acknowledgements. This work was assisted by the Australian Government's Cooperative Research Centres Programme, through the Antarctic Climate and Ecosystems Cooperative Research Centre. Funding support in France was provided by the LEFE programme of the Institut National des Sciences de l'Univers (INSU) and by the project ANR-07-BLAN-0125 of Agence Nationale de la Recherche. S.O.R. was supported by an Inge Lehmann grant.

References

- Andersen, K. K., Ditlevsen, P. D., Rasmussen, S. O., Clausen, H. B., Vinther, B. M., Johnsen, S. J., and Steffensen, J. P.: Retrieving a common accumulation record from Greenland ice cores for the past 1800 years, *J. Geophys. Res.*, 111, D15106, doi:10.1029/2005JD006765, 2006a.
- Andersen, K. K., Svensson, A., Johnsen, S. J., Rasmussen, S. O., Bigler, M., Rothlisberger, R., Ruth, U., Siggaard-Andersen, M., Peder Steffensen, J., Dahl-Jensen, D., Vinther, B. M., and Clausen, H. B.: The Greenland Ice Core Chronology 2005, 15 42 ka. Part 1: constructing the time scale, *Quaternary Science Reviews*, 25, 3246-3257, doi:10.1016/j.quascirev.2006.08.002, 2006b.
- Anderson, R. F., Ali, S., Bradtmiller, L. I., Nielsen, S. H. H., Fleisher, M. Q., Anderson, B. E., and Burckle, L. H.: Wind-Driven Upwelling in the Southern Ocean and the Deglacial Rise in Atmospheric CO₂, *Science*, 323, 1143–1448, 2009.
- Barker, S., Knorr, G., Vautravers, M. J., Diz, P., and Skinner, L. C.: Extreme deepening of the Atlantic circulation during deglaciation, *Nat. Geosci.*, 3, 567–571, 2010.
- Barnola, J. M., Pimienta, P., Raynaud, D., and Korotkevich, Y. S.: CO₂-climate relationship as deduced from the Vostok ice core: a re-examination based on new measurements and on a re-evaluation of the air dating, *Tellus Ser. B.*, 43, 83–90, 1991.
- Bianchi, C. and Gersonde, R.: Climate evolution at the last deglaciation: the role of the Southern Ocean, *Earth Planet. Sci. Lett.*, 228, 407–424, 2004.
- Blunier, T. and Brook, E. J.: Timing of millennial-scale climate change in Antarctica and Greenland during the last glacial period, *Science*, 291, 109–112, 2001.
- Blunier, T., Chappellaz, J., Schwander, J., Dällenbach, A., Stauffer, B., Stocker, T. F., Raynaud, D., Jouzel, J., Clausen, H. B., Hammer, C. U., and Johnsen, S. J.: Asynchrony of Antarctic and Greenland climate change during the last glacial period, *Nature*, 394, 739–743 1998.
- Broecker, W.: Palaeocean circulation during the last deglaciation: A bipolar seesaw?, *Paleoceanography*, 13, 119–121, 1998.
- Brook, E. J., White, J. W. C., Schilla, A. S. M., Bender, M. L., Barnett, B. Severinghaus, J. P., Taylor, K. C., Alley, R. B., and Steig, E. J.: Timing of millennial-scale climate change at Siple Dome, West Antarctica, during the last glacial period, *Quat. Sci. Rev.*, 24, 1333–1343, 2005.
- Buiron, D., Chappellaz, J., Stenni, B., Frezzotti, M., Baumgartner, M., Capron, E., Landais, A., Lemieux-Dudon, B., Masson-Delmotte, V., Montagnat, M., Parrenin, F., and Schilt, A.:

The last deglaciation: timing the bipolar seesaw

J. B. Pedro et al.

Title Page

Abstract

Introduction

Conclusions

References

Tables

Figures



Back

Close

Full Screen / Esc

Printer-friendly Version

Interactive Discussion



The last deglaciation: timing the bipolar seesaw

J. B. Pedro et al.

Title Page

Abstract

Introduction

Conclusions

References

Tables

Figures

◀

▶

◀

▶

Back

Close

Full Screen / Esc

Printer-friendly Version

Interactive Discussion



TALDICE-1 age scale of the Talos Dome deep ice core, East Antarctica, *Clim. Past*, 7, 1–16, doi:10.5194/cp-7-1-2011, 2011.

Chaudhuri, P. and Marron, J. S.: SiZer for Exploration of Structures in Curves, *J. Am. Stat. Assoc.*, 94, 807–823, 1999. (A SiZer script for MatLab can be obtained from http://www.unc.edu/~marron/marron_software.html).

Delmotte, M., Raynaud, D., Morgan, V., and Jouzel, J.: Climatic and glaciological information inferred from air content measurements of a Law Dome (East Antarctica) ice core, *J. Glaciol.*, 45, 255–263, 1999.

Denton, G. H., Anderson, R. F., Toggweiler, J. R., Edwards, R. L., Schaefer, J. M., and Putnam, A. E.: The last glacial termination, *Science*, 328, 1652–1656, 2010.

EPICA community members: One-to-one coupling of glacial climate variability in Greenland and Antarctica, *Nature*, 444, 195–198, 2006.

Ganopolski, A. and Rahmstorf, S.: Rapid changes of glacial climate simulated in a coupled climate model, *Nature*, 409, 153–158, 2001.

Goujon, C., Barnola, J.-M., and Ritz, C.: Modeling the densification of polar firn including heat diffusion: Application to close-off characteristics and gas isotopic fractionation for Antarctica and Greenland sites, *J. Geophys. Res.*, 108, 4792, doi:10.1029/2002JD003319, 2003.

Johnsen, S. J., Clausen, H. B., Dansgaard, W., Gundestrup, N. S., Hammer, C. U., Andersen, U., Andersen, K. K., Hvidberg, C. S., Dahl-Jensen, D., Steffensen, J. P., Shoji, H., Sveinbjörnsdóttir, Á. E., White, J., Jouzel, J., and Fisher, D.: The $\delta^{18}\text{O}$ record along the Greenland Ice Core Project deep ice core and the problem of possible Eemian climatic instability, *J. Geophys. Res.*, 102, 26397–26410, doi:10.1029/97JC00167, 1997.

Jones, P. D., Briffa, K. R., Osborn, T. J., Lough, J. M., van Ommen, T. D., Vinther, B. M., Luterbacher, J., Wahl, E. R., Zwiwers, F. W., Mann, M. E., Schmidt, G. A., Ammann, C. M., Buckley, B. M., Cobb, K. M., Esper, J., Goosse, H., Graham, N., Jansen, E., Kiefer, T., Kull, C., Küttel, M., Mosley-Thompson, E., Overpeck, J. T., Riedwyl, N., Schulz, M., Tudhope, A. W., Villalba, R., Wanner, H., Wolff, E., and Xoplaki, E.: High-resolution paleoclimatology of the last millennium: a review of current status and future prospects, *Holocene*, 19, 3–49, 2009.

Jouzel, J., Masson, V., Cattani, O., Falourd, S., Stievenard, M., Stenni, B., Longinelli, A., Johnsen, S. J., Steffenssen, J. P., Petit, J. R., Schwander, J., Souchez, R., and Barkov, N. I.: A new 27 ky high resolution East Antarctic climate record, *Geophys. Res. Lett.*, 28, 3199–3202, doi:10.1029/2000GL012243, 2001.

**The last deglaciation:
timing the bipolar
seesaw**J. B. Pedro et al.

[Title Page](#)[Abstract](#)[Introduction](#)[Conclusions](#)[References](#)[Tables](#)[Figures](#)[Back](#)[Close](#)[Full Screen / Esc](#)[Printer-friendly Version](#)[Interactive Discussion](#)

- Kaplan, M. R., Schaefer, J. M., Denton, G. H., Barrell, D. J. A., Chinn, T. J. H., Putnam, A. E., Andersen, B. G., Finkel, R. C., Schwartz, R., and Doughty, A. M.: Glacier retreat in New Zealand during the Younger Dryas stadial, *Nature*, 467, 194–197, 2010.
- Knorr, G. and Lohmann, G.: Southern Ocean origin for the resumption of Atlantic thermohaline circulation during deglaciation, *Nature*, 424, 532–535, 2003.
- Landais, A., Barnola, J. M., Kawamura, K., Caillon, N., Delmotte, M., van Ommen, T., Dreyfus, G., Jouzel, J., Masson-Delmotte, V., Minster, B., Freitag, J., Leuenberger, M., Schwander, J., Huber, C., Etheridge, D., and Morgan, V.: Firn-air $\delta^{15}\text{N}$ in modern polar sites and glacial interglacial ice: a model-data mismatch during glacial periods in Antarctica?, *Quaternary Science Reviews*, 25, 49–62, doi:10.1016/j.quascirev.2005.06.007, 2006.
- Lemieux-Dudon, B., Blayo, E., Petit, J.-R., Waelbroeck, C., Svensson, A., Ritz, C., Barnola, J.-M., Narcisi, B. M., and Parrenin, F.: Consistent dating for Antarctic and Greenland ice cores, *Quat. Sci. Rev.*, 29, 8–20, 2010.
- Liu, Z., Otto-Bliesner, B. L., He, F., Brady, E. C., Tomas, R., Clark, P. U., Carlson, A. E., Lynch-Stieglitz, J., Curry, W., Brook, E., Erickson, D., Jacob, R., Kutzbach, J., and Cheng, J.: Transient Simulation of Last Deglaciation with a New Mechanism for Bølling-Allerød Warming, *Science*, 325, 310–314, doi:10.1126/science.1171041, 2009.
- Loulergue, L., Parrenin, F., Blunier, T., Barnola, J.-M., Spahni, R., Schilt, A., Raisbeck, G., and Chappellaz, J.: New constraints on the gas age-ice age difference along the EPICA ice cores, 0–50 kyr, *Clim. Past*, 3, 527–540, doi:10.5194/cp-3-527-2007, 2007.
- Lowe, J. J., Rasmussen, S. O., Björck, S., Hoek, W. Z., Steffensen, J. P., Walker, M. J. C., and Yu, Z. C.: Synchronisation of palaeoenvironmental events in the North Atlantic region during the Last Termination: a revised protocol recommended by the INTIMATE group, *Quat. Sci. Rev.*, 27, 6–17, 2008.
- Lucas, M. A., Hirschi, J. J.-M., and Marotzke, J.: Response of the meridional overturning circulation to variable buoyancy forcing in a double hemisphere basin, *Clim. Dyn.*, 34, 615–627, 2010.
- Masuda, S., Awaji, T., Sugiura, N., Matthews, J. P., Toyoda, T., Kawai, Y., Doi, T., Kouketsu, S., Igarashi, H., Katsumata, K., Uchida, H., Kawano, T., and Fukasawa, M.: Simulated Rapid Warming of Abyssal North Pacific Waters, *Science*, 329, 319–322, doi:10.1126/science.1188703, 2010.
- McManus, J. F., Francois, R., Gherardi, J.-M., Keigwin, L. D., and Brown-Leger, S.: Collapse and rapid resumption of Atlantic meridional circulation linked to deglacial climate changes,

The last deglaciation: timing the bipolar seesaw

J. B. Pedro et al.

Title Page

Abstract

Introduction

Conclusions

References

Tables

Figures



Back

Close

Full Screen / Esc

Printer-friendly Version

Interactive Discussion



Nature, 428, 834–837, 2004.

Meese, D. A., Gow, A. J., Alley, R. B., Zielinski, G. A., Grootes, P. M., Ram, M., Taylor, K. C., Mayewski, P. A., and Bolzan, J. F.: The Greenland Ice Sheet Project 2 depth-age scale: Methods and results, *J. Geophys. Res.*, 102, 26 411–26 424, doi:10.1029/97JC00269, 1997.

5 Monnin, E., Steig, E. J., Siegenthaler, U., Kawamura, K., Schwander, J., Stauffer, B., Stocker, T. F., Morse, D. L., Barnola, J.-M., Bellier, B., Raynaud, D., and Fischer, H.: Evidence for substantial accumulation rate variability in Antarctica during the Holocene, through synchronization of CO₂ in the Taylor Dome, Dome C and DML ice cores, *Earth and Planetary Science Letters*, 224, 45–54, doi:10.1016/j.epsl.2004.05.007, 2004.

10 Morgan, V., Delmotte, M., van Ommen, T. D., Jouzel, J., Chappellaz, J., Woon, S., Masson-Delmotte, V., and Raynaud, D.: Relative timing of deglacial climate events in Antarctica and Greenland, *Science*, 297, 1862–1864, 2002.

NGRIP members: High-resolution record of Northern Hemisphere climate extending into the Last Interglacial period, *Nature*, 431, 147–151, 2004.

15 Noone, D. and Simmonds, I.: The sea ice control on water isotope transport to Antarctica and implications for ice core interpretation, *J. Geophys. Res.*, 109, D07105, doi:10.1029/2003JD004228, 2004.

Parrenin, F., Barnola, J.-M., Beer, J., Blunier, T., Castellano, E., Chappellaz, J., Dreyfus, G., Fischer, H., Fujita, S., Jouzel, J., Kawamura, K., Lemieux-Dudon, B., Loulergue, L., Masson-Delmotte, V., Narcisi, B., Petit, J.-R., Raisbeck, G., Raynaud, D., Ruth, U., Schwander, J., Severi, M., Spahni, R., Steffensen, J. P., Svensson, A., Udisti, R., Waelbroeck, C., and Wolff, E.: The EDC3 chronology for the EPICA Dome C ice core, *Clim. Past*, 3, 485–497, doi:10.5194/cp-3-485-2007, 2007.

20 Rasmussen, S. O., Seierstad, I. K., Andersen, K. K., Bigler, M., Dahl-Jensen, D., and Johnsen, S. J.: Synchronization of the NGRIP, GRIP, and GISP2 ice cores across MIS 2 and palaeoclimatic implications, *Quaternary Science Reviews*, 27, 18–28, doi:10.1016/j.quascirev.2007.01.016, 2008.

25 Rasmussen S. O., Seierstad, I. K., Andersen, K. K., Bigler, M., Dahl-Jensen, D., and Johnsen, S. J.: Synchronization of the NGRIP, GRIP, and GISP2 ice cores across MIS 2 and palaeoclimatic implications, *Quat. Sci. Rev.*, 27, 18–28, 2008.

30 Shakun, J. D. and Carlson, A. E.: A global perspective on Last Glacial Maximum to Holocene climate change, *Quat. Sci. Rev.*, 29, 1801–1816, 2010.

Sowers, T. and Bender, M.: Climate records covering the last deglaciation, *Science*, 269, 210–

214, 1995.

Stanford, J. D., Rohling, E. J., Hunter, S. E., Roberts, A. P., Rasmussen, S. O., Bard, E., McManus, J., and Fairbanks, R. G.: Timing of meltwater pulse 1a and climate responses to meltwater injections, *Paleoceanography*, 21, doi:10.1029/2006PA001340, 2006.

5 Steffensen, J. P., Andersen, K. K., Bigler, M., Clausen, H. B., Dahl-Jensen, D., Fischer, H., Goto-Azuma, K., Hansson, M., Johnsen, S. J., Jouzel, J., Masson-Delmotte, V., Popp, T., Rasmussen, S. O., Röthlisberger, R., Ruth, U., Stauffer, B., Siggaard-Andersen, M., Sveinbjörnsdóttir, Á . E., Svensson, A., and White, J. W. C.: High-Resolution Greenland Ice Core Data Show Abrupt Climate Change Happens in Few Years, *Science*, 321, 680-684, doi:10.1126/science.1157707, 2008.

10 Stenni, B., Buiron, D., Frezzotti, M., Albani, S., Barbante, C., Bard, E., Barnola, J. M., Baroni, M., Baumgartner, M., Bonazza, M., Capron, E., Castellano, E., Chappellaz, J., Delmonte, B., Falourd, S., Genoni, L., Iacumin, P., Jouzel, J., Kipfstuhl, S., Landais, A., Lemieux-Dudon, B., Maggi, V., Masson-Delmotte, V., Mazzola, C., Minster, B., Montagnat, M., Mulvaney, R.,
15 Narcisi, B., Oerter, H., Parrenin, F., Petit, J. R., Ritz, C., Scarchilli, C., Schilt, A., Schúpbach, S., Schwander, J., Selmo, E., Severi, M., Stocker, T. F., and Udisti, R.: Expression of the bipolar see-saw in Antarctic climate records during the last deglaciation, *Nature Geoscience*, 4, 46-49, doi:10.1038/ngeo1026, 2011.

20 Stocker, T. F. and Johnsen, S. J.: A minimum thermodynamic model for the bipolar seesaw, *Paleoceanography* 18, PA000920, doi:10.1029/2003PA000920, 2003.

Stouffer, R. J., Seidov, D., and Haupt, B. J.: Climate response to external sources of freshwater: North Atlantic versus the Southern Ocean, *J. Climate*, 20(3), 436–448, 2007.

25 Swingedouw, D., Fichet, T., Goosse, H., and Loutre, M. F.: Impact of transient freshwater releases in the Southern Ocean on the AMOC and climate, *Clim. Dyn.*, 33, 365–381, doi:10.1007/s00382-008-0496-1, 2009.

Thornalley, D. J. R., McCave, I. N., and Elderfield, H.: Freshwater input and abrupt deglacial climate change in the North Atlantic, *Palaeoceanography*, 25, PA1201, doi:10.1029/2009PA001772, 2010.

30 Timmermann, R., Le Brocq, A., Deen, T., Domack, E., Dutrieux, P., Galton-Fenzi, B., Hellmer, H., Humbert, A., Jansen, D., Jenkins, A., Lambrecht, A., Makinson, K., Niederjasper, F., Nitsche, F., Nøst, O. A., Smedsrud, L. H., and Smith, W. H. F.: A consistent data set of Antarctic ice sheet topography, cavity geometry, and global bathymetry, *Earth Syst. Sci. Data*, 2, 261–273, doi:10.5194/essd-2-261-2010, 2010.

The last deglaciation: timing the bipolar seesaw

J. B. Pedro et al.

Title Page

Abstract

Introduction

Conclusions

References

Tables

Figures

◀

▶

◀

▶

Back

Close

Full Screen / Esc

Printer-friendly Version

Interactive Discussion



van Ommen, T. D. and Morgan V. I.: Calibrating the ice core paleothermometer using seasonality, *J. Geophys. Res.*, 102, 9351–9357, 1997.

van Ommen, T. D., Morgan V. I., and Curran M. A. J.: Deglacial and Holocene changes in accumulation at Law Dome, edited by: Jacka, T. H., *Ann. Glaciol.*, 39, 359–365, 2004.

5 Weaver, A. J., Saenko, O. A., Clark, P. U., and Mitrovica, J. X. Meltwater Pulse 1A from Antarctica as a Trigger of the Bølling-Allerød Warm Interval, *Science*, 299, 1709–1713, 2003.

White, J. W. C., Barlow, L. K., Fisher, D., Grootes, P., Jouzel, J., Johnsen, S. J., Stuiver, M., and Clausen, H.: The climate signal in the stable isotopes of snow from Summit, Greenland: results of comparisons with modern climate observations, *J. Geophys. Res.*, 102(26), 425–

10 39, 1997.

CPD

7, 397–430, 2011

The last deglaciation: timing the bipolar seesaw

J. B. Pedro et al.

Title Page

Abstract

Introduction

Conclusions

References

Tables

Figures

◀

▶

◀

▶

Back

Close

Full Screen / Esc

Printer-friendly Version

Interactive Discussion



The last deglaciation: timing the bipolar seesaw

J. B. Pedro et al.

Title Page

Abstract

Introduction

Conclusions

References

Tables

Figures

◀

▶

◀

▶

Back

Close

Full Screen / Esc

Printer-friendly Version

Interactive Discussion



Table 1. Site characteristics and Δ age values during modern, ACR and LGM times at the Antarctic ice core sites mentioned in the text.

Site	Location	Elevation (m a.s.l.)	Distance from ocean ^d (km)	Δ age modern (yr)	Δ age at ACR (yr)	Δ age at LGM (yr)
LD	66°46′ S, 112°48′ E	1370	100	60	350	700
Byrd ^a	80°01′ S, 119°31′ W	1530	591	270	380	480
Siple ^b	81°40′ S, 148°49′ W	621	439	242	381	815
Talos ^c	72°49′ S, 159°11′ E	2315	250	675	920	1595
EDML ^d	75°00′ S, 00°04′ E	2892	577	800	1200	2300
EDC ^e	74°39′ S, 124°10′ E	3240	912	2400	3000	4500
Vostok ^f	78°28′ S, 106°48′ E	3490	1409	3300	4400	5200

Source of Δ age and elevation data:

^a Blunier and Brook (2001)

^b Brook et al. (2005)

^c Stenni et al. (2011)

^d Lemieux-Dudon et al. (2010)

^e Parrenin et al. (2007)

^f Goujon et al. (2003)

^g Timmermann et al. (2010) (with ice shelves considered part of the continent)

The last deglaciation: timing the bipolar seesaw

J. B. Pedro et al.

Table 2. LD age ties used in construction of the deglacial chronology and their uncertainties.

Type	LD depth (m)	LD GICC05 gas age $\pm\sigma_{\text{correl}}$ (ka b1950)	$\Delta\text{age} \pm\sigma_{\Delta\text{age}}$ (yr)	LD ice age $\pm\sigma_{\text{ice}}$ (ka b1950)
$\delta^{18}\text{O}_{\text{air}}$	1108.64	09.30 \pm 0.15	119 \pm 36	9.42 \pm 0.15
CH ₄ : Start of Holocene	1121.29	11.63 \pm 0.75	143 \pm 43	11.78 \pm 0.90
CH ₄ : Start of GS-1	1125.19	12.77 \pm 0.10	272 \pm 82	13.04 \pm 0.13
CH ₄ : Start of GI-1e	1129.04	14.64 \pm 0.30	298 \pm 89	14.94 \pm 0.10
CH ₄ : Start of deglacial rise	1131.75	15.67 \pm 0.30	420 \pm 125	16.09 \pm 0.32
CH ₄ : DO7	1144.28	35.34 \pm 0.18	540 \pm 160	35.88 \pm 0.25
CH ₄ : DO8	1146.70	38.34 \pm 0.20	500 \pm 150	38.84 \pm 0.25

σ_{correl} refers to the uncertainty involved in correlating the LD CH₄ record with the GISP2 CH₄ record; $\sigma_{\Delta\text{age}}$ refers to the uncertainty in Δage at LD; and σ_{ice} is calculated as the RMS sum of σ_{correl} and $\sigma_{\Delta\text{age}}$.

Title Page

Abstract

Introduction

Conclusions

References

Tables

Figures

◀

▶

◀

▶

Back

Close

Full Screen / Esc

Printer-friendly Version

Interactive Discussion



The last deglaciation: timing the bipolar seesaw

J. B. Pedro et al.

Table 3. Dating uncertainties in the individual records used in the Antarctic composite during the deglaciation (Sect. 2.4)

Core	Late deglaciation (~ 10–13 ka)			Middle deglaciation (~ 13–15 ka)			Early deglaciation (~ 15–18 ka)		
	σ_{correl}	$\sigma_{\Delta\text{age}}$	σ_{ice}	σ_{correl}	$\sigma_{\Delta\text{age}}$	σ_{ice}	σ_{correl}	$\sigma_{\Delta\text{age}}$	σ_{ice}
LD	100	80	128	30	90	95	300	125	325
Byrd ^a	200	200	283	200	200	283	300	200	361
Siple Dome ^b	170	110	202	120	130	177	320	190	372
Talos ^c	–	–	300	–	–	300	–	–	500
EDML ^d	–	–	200	–	–	140	–	–	360
Average	–	–	223	–	–	199	–	–	384

^a Blunier and Brook (2001)

^b Brook et al. (2005)

^c Buiron et al. (2011)

^d Lemieux-Dudon et al. (2010)

Title Page

Abstract

Introduction

Conclusions

References

Tables

Figures

◀

▶

◀

▶

Back

Close

Full Screen / Esc

Printer-friendly Version

Interactive Discussion



The last deglaciation: timing the bipolar seesaw

J. B. Pedro et al.

Table 4. The timing of climate features in the LD and Antarctic composite $\delta^{18}\text{O}$ records derived from SiZer analysis. Dating uncertainties are the RMS sum of the dating uncertainty and uncertainty in the statistical method for picking timing of the climate feature (Sect. 2.3).

Climate feature	LD Age (ka b1950)	Composite Age (ka b1950)
Start deglacial warming	17.92 ± 0.33	18.00 ± 0.39
End warming (earliest ACR onset)	15.11 ± 0.16	14.76 ± 0.20
Start cooling (latest ACR onset)	14.74 ± 0.10	14.62 ± 0.20
End cooling (earliest ACR termination)	14.30 ± 0.11	14.08 ± 0.20
Start warming (latest ACR termination)	14.02 ± 0.11	13.18 ± 0.21
End deglacial warming	9.68 ± 0.15	11.68 ± 0.23

Title Page

Abstract

Introduction

Conclusions

References

Tables

Figures

◀

▶

◀

▶

Back

Close

Full Screen / Esc

Printer-friendly Version

Interactive Discussion



The last deglaciation: timing the bipolar seesaw

J. B. Pedro et al.

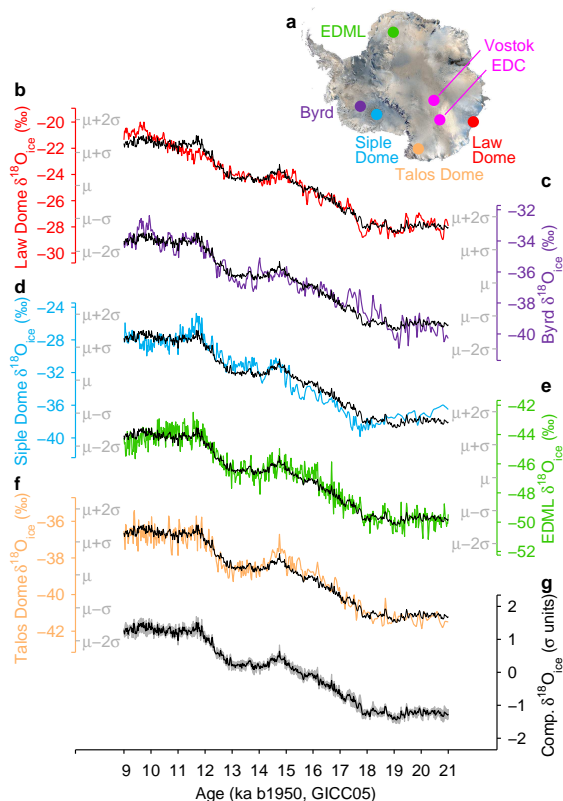


Fig. 1. $\delta^{18}\text{O}_{\text{ice}}$ records from high-accumulation/near-coastal sites used to construct the Antarctic composite. **(a)**, Map showing the location of the ice cores used and other records mentioned in the text (source: NASA). **(b)–(f)**, deglacial $\delta^{18}\text{O}_{\text{ice}}$ records from LD, Byrd, Siple Dome, Talos Dome and EDML all placed on the common GICC05 timescale; the individual vertical axes are scaled according to the standard deviation of each record, as can be seen from the inner σ axis labels (in grey). **(g)**, the Antarctic composite $\delta^{18}\text{O}_{\text{ice}}$ (black, also overlain in panels b–e) is shown bracketed by the standard error in the mean of the $\delta^{18}\text{O}_{\text{ice}}$ records from the five sites (grey shading). Estimated dating uncertainty in the composite (relative to GICC05) is 380 yr, 200 yr and 220 yr for intervals 15–18 ka, 13–15 ka and 10–13 ka respectively.

Title Page

Abstract

Introduction

Conclusions

References

Tables

Figures

◀

▶

◀

▶

Back

Close

Full Screen / Esc

Printer-friendly Version

Interactive Discussion



The last deglaciation: timing the bipolar seesaw

J. B. Pedro et al.

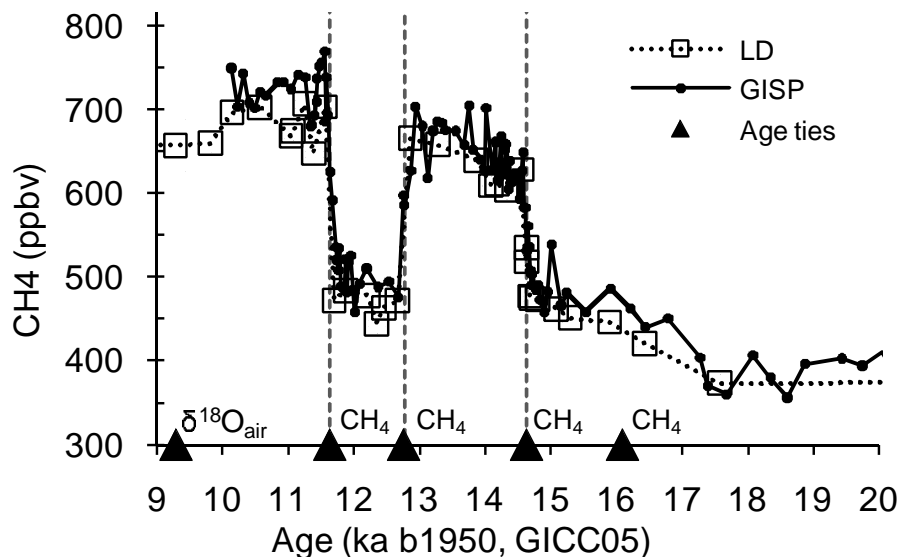


Fig. 2. Dating of the LD ice core through the deglaciation. LD methane is synchronised with GISP2 methane (Blunier and Brook, 2001) on the GICC05 timescale. Timing of methane transitions at the onset of the Bølling, Younger Dryas and Holocene are shown as dashed vertical lines. Triangles mark the position and type of the dating ties used through the deglaciation. Standard error in LD methane concentrations are ≤ 20 ppm.

Title Page

Abstract

Introduction

Conclusions

References

Tables

Figures

◀

▶

◀

▶

Back

Close

Full Screen / Esc

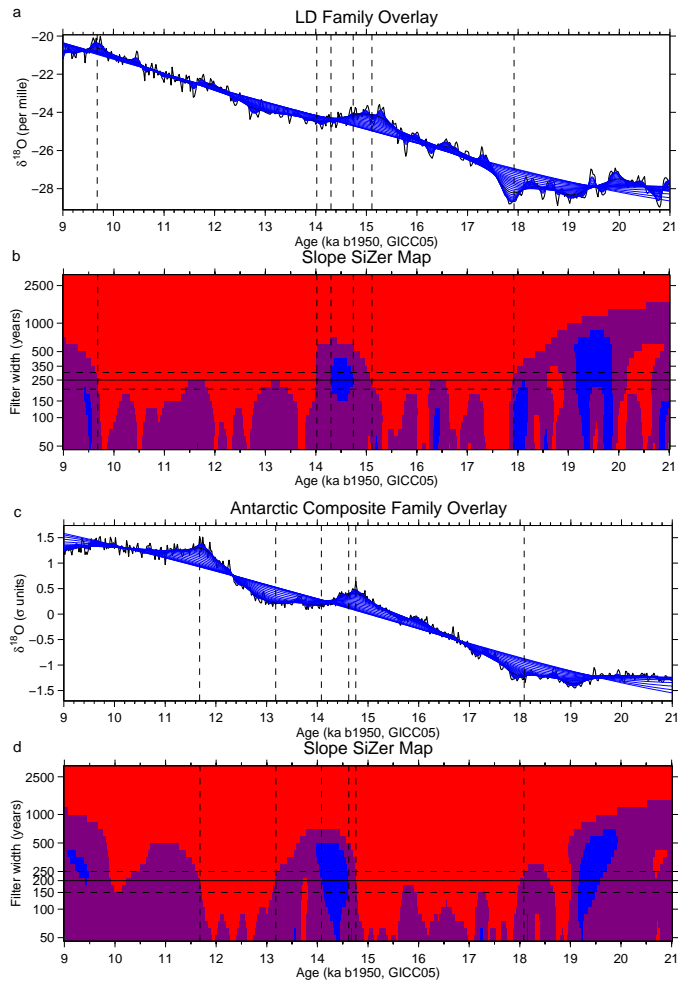
Printer-friendly Version

Interactive Discussion



The last deglaciation: timing the bipolar seesaw

J. B. Pedro et al.



Title Page

Abstract

Introduction

Conclusions

References

Tables

Figures



Back

Close

Full Screen / Esc

Printer-friendly Version

Interactive Discussion



The last deglaciation: timing the bipolar seesaw

J. B. Pedro et al.

Fig. 3. “SiZer maps” of the significance of features in LD $\delta^{18}\text{O}_{\text{ice}}$ and the Antarctic composite through the deglaciation. **(a)**, “LD Family Overlay”: the series of blue curves shows LD $\delta^{18}\text{O}_{\text{ice}}$ smoothed across a range of filter widths from 40 to 3000 yr whilst the black curves shows the original data and the data smoothed with a filter width of 250 yr. **(b)**, “LD Slope Sizer Map”: the significance and sign of the slope of the smoothed data is shown as the filter width (on the vertical axis) is varied; red signifies significant positive slope (warming), blue signifies significant negative slope (cooling) and purple signifies regions where the slope is not statistically different from zero (all with respect to the 95% CL); for instance, the significant cooling during the ACR appears as the blue area in the centre of the figure. The timing of significant climate features is interpreted from the intercepts of the 250 ± 50 yr smooth (horizontal line and dashed lines) with the changes in the significance and/or sign of the slope. Significant features are marked with dashed vertical lines. The timing and dating uncertainty of climate features are listed in Table 4. **(c)**, “Antarctic Composite Family Overlay” interpret as above. **(d)**, “Antarctic composite Slope SiZer Map” the timing of significant climate features is interpreted from the intercepts of the 200 ± 50 yr smooth with the changes in the significance and/or sign of the slope.

Title Page

Abstract

Introduction

Conclusions

References

Tables

Figures

◀

▶

◀

▶

Back

Close

Full Screen / Esc

Printer-friendly Version

Interactive Discussion



The last deglaciation: timing the bipolar seesaw

J. B. Pedro et al.

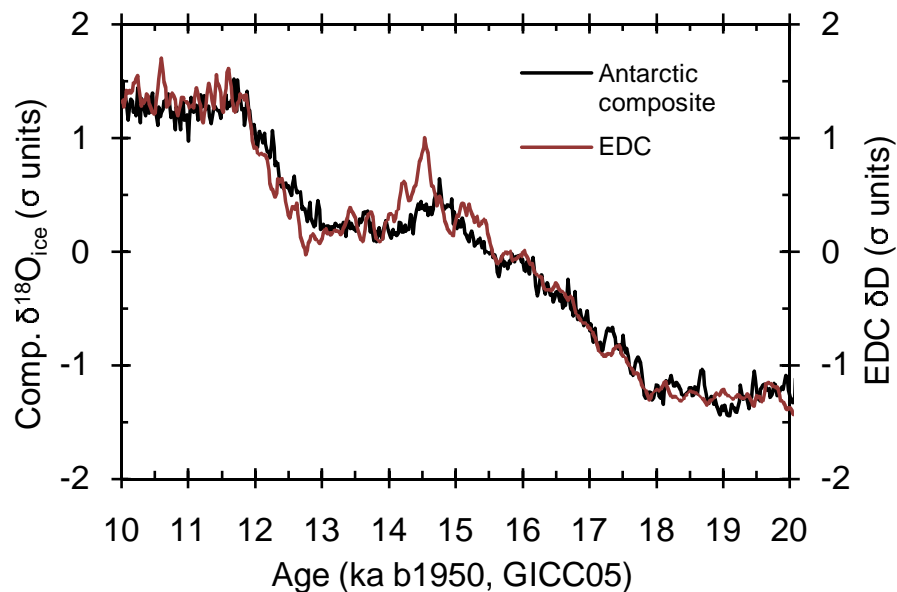


Fig. 4. A comparison of the Antarctic composite with the EPICA Dome C (EDC) $\delta^2\text{H}_{\text{ice}}$ record. The GICC05 consistent timescale for EDC is from Lemieux-Dudon et al. (2010) and $\delta^2\text{H}_{\text{ice}}$ data are from Jouzel et al. (2001).

[Title Page](#)[Abstract](#)[Introduction](#)[Conclusions](#)[References](#)[Tables](#)[Figures](#)[◀](#)[▶](#)[◀](#)[▶](#)[Back](#)[Close](#)[Full Screen / Esc](#)[Printer-friendly Version](#)[Interactive Discussion](#)

The last deglaciation: timing the bipolar seesaw

J. B. Pedro et al.

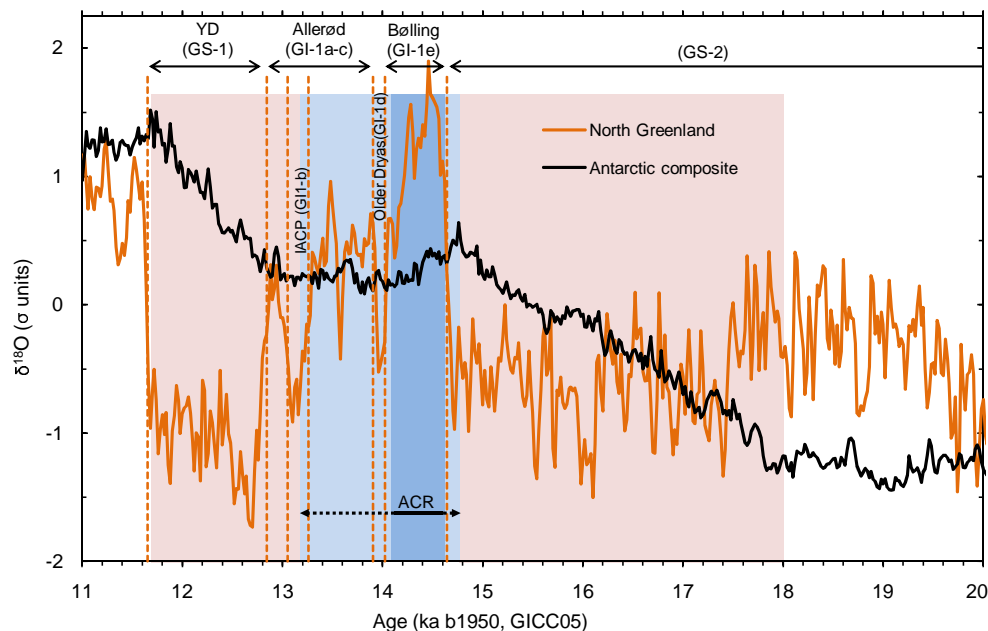


Fig. 5. A comparison of the pattern and timing of climate change in the Antarctic and North Atlantic regions during the last deglaciation. The Antarctic composite $\delta^{18}\text{O}_{\text{ice}}$ record and the North Greenland (NGRIP) $\delta^{18}\text{O}_{\text{ice}}$ record. Vertical pink bands correspond to periods of significant Antarctic warming, vertical light blue bands correspond to a pause in Antarctic warming and the vertical dark blue band corresponds to significant Antarctic cooling. The minimum duration of the ACR is the period spanned by the dark blue band, the maximum duration of the ACR also includes the periods spanned by the light blue bands (as marked by the solid and dashed horizontal lines below the ACR label). Dashed vertical orange lines and labels at the top of the figure show the exact timing of the North Atlantic INTIMATE climate stages (Lowe et al., 2008).

Title Page

Abstract

Introduction

Conclusions

References

Tables

Figures

⏪

⏩

◀

▶

Back

Close

Full Screen / Esc

Printer-friendly Version

Interactive Discussion



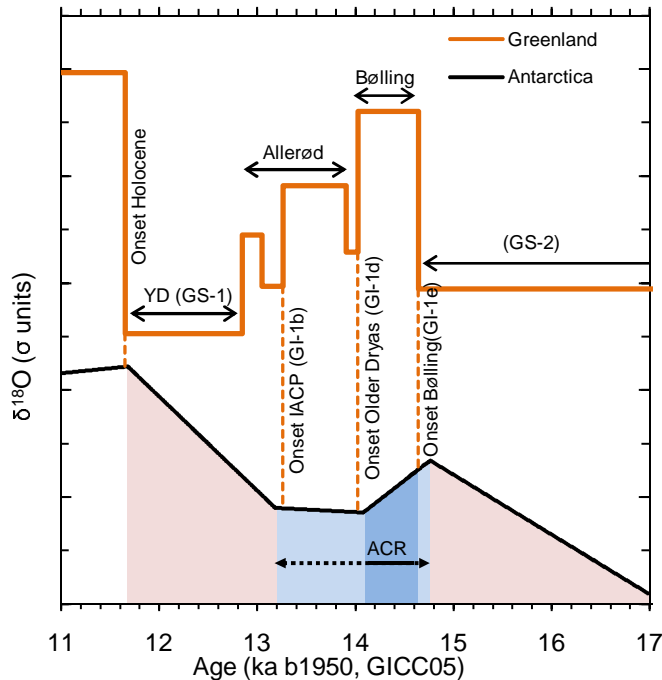


Fig. 6. A schematic view of the observed north-south climate coupling on millennial and sub-millennial timescales during the deglaciation. The Antarctic composite curve is simplified by linearly interpolating between the timing and $\delta^{18}\text{O}_{\text{ice}}$ values of the points of significant change in $\delta^{18}\text{O}_{\text{ice}}$ trends; colour shading as in Fig. 2. The North Greenland (NGRIP) curve is simplified by averaging the $\delta^{18}\text{O}_{\text{ice}}$ values during each of the North Atlantic INTIMATE climate stages (Lowe et al., 2008); the general climate deterioration through the Bølling-Allerød is apparent, as are the near-stadial conditions reached during the sub millennial Intra-Allerød Cold Period (IACP).

**The last deglaciation:
timing the bipolar
seesaw**

J. B. Pedro et al.

Title Page

Abstract Introduction

Conclusions References

Tables Figures

◀ ▶

◀ ▶

Back Close

Full Screen / Esc

Printer-friendly Version

Interactive Discussion

